Published in IET Generation, Transmission & Distribution
Received on 28th March 2010
Revised on 11th September 2010
doi: 10.1049/iet-gtd.2010.0215

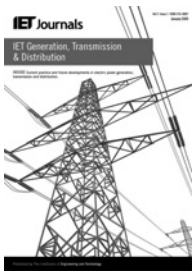

ISSN 1751-8687

Optimal coordination of stochastic hydro and natural gas supplies in midterm operation of power systems

L. Wu[1] *M. Shahidehpour*[2]

[1]*Electrical and Computer Engineering Department, Clarkson University Potsdam, New York, USA*
[2]*Electrical and Computer Engineering Department, Illinois Institute of Technology, Chicago, Illinois, USA*
E-mail: ms@iit.edu

Abstract: This study presents a stochastic security-constrained unit commitment (SCUC) model for the optimisation of coordinated midterm water and natural gas supplies. The stochastic model considers random outages of system components, load forecast errors and water inflow uncertainty, which are modelled as scenarios in the Monte Carlo simulation. Water resources may be used in winter to cover gas unit outages caused by an insufficient gas supply. However, those hydro units then may not be available for peak load shaving in the following summer if the summer happens to be a dry season. Thus, water reservoirs would have to be utilised efficiently throughout the year to provide substantial cost reductions while maintaining the power system reliability. The proposed model also considers the impact of midterm security-constrained scheduling of water and gas on the power system reliability. Accordingly, hourly SCUC is incorporated in the reliability calculation. The proposed stochastic problem is formulated as a two-stage optimisation in which the first stage optimises the water and gas usages in the first month and the second stage considers the schedule via multiple scenarios in the following 11 months. Numerical simulations indicate the effectiveness of the proposed stochastic approach for the optimal scheduling of midterm water and gas usages.

Nomenclature

Variables

b, c	index of bus/catchment
$F_c(\cdot)$	production cost function of a unit
h, i	index of hydro/thermal unit
I^s_{itp}, P^s_{itp}	commitment state and real power generation of thermal unit i at time t at period p in scenario s
j, k	index of iteration
$\mathrm{LS}^s_{btp,\,m}$	load shedding quantity of contract m at bus b at time t at period p in scenario s
m	index of curve segments
p, t	index of period, and hours in each period
SU^s_{itp}, SD^s_{itp}	startup/shutdown cost of thermal unit i at time t at period p in scenario s
V^s_{htp}	reservoir volume of hydro unit h at time t at period p in scenario s
β	Lagrangian multiplier
γ^s_{ctp}	global parameter for catchment c describing its depletion policy at time t at period p in scenario s
$\gamma_{h,m}$	global parameter corresponding to hydro unit h at segment m in linearised depletion curve
$\delta_{h,m}$	indicates whether hydro unit h is operated at segment m in linearised depletion curve
$v_{h,m}$	volume of segment m in linearised depletion curve for hydro unit h

Constants

$\mathrm{IC}_{h,m}$	slope of segment m in linearised depletion curve for hydro unit h
NB, NC	number of buses/catchments
NG, NH	number of thermal/hydro units
NH_c	number of hydro units belongs to catchment c
NPD, NPS	number of periods at the first/second stage under study
NM_b	number load shedding contracts at bus b
NS	number of scenarios
NT	number of hours at each period
p^s	probability of scenario s
PL^s_{tp}	system load at time t at period p in scenario s
$pv^s_{b,\,m}$	value of lost load (VOLL) corresponding to segment m of bus b in scenario s
$V_{h,\max}$, $V_{h,\min}$	upper/lower limit of reservoir volume of hydro unit h

$V_{h,\,m}$ upper volume limit of segment m in linearised depletion curve for hydro unit h

Note: Corresponding variables are also considered for hydro units by changing index i to h.

1 Introduction

In restructured power systems, independent system operators (ISOs) maintain the power system reliability when supplying the hourly load at minimum cost [1]. In this environment, the interdependency of natural gas and electric power systems could affect the security and the economics of power systems. For instance, in winter months when residential usages of gas increases in some regions, there may be an insufficient level of gas available for gas-fired generating units. Hydro units could be used in such occasions in order to avoid electric load curtailments. However, if the following spring season happens to be dry, water reservoirs utilised in the previous winter would not be replenished. Thus, insufficient water resources could lead to the inability of hydro units to supply summer peak loads. In order to minimise peak load curtailments in the coming summer months, water usage has to be limited in the winter by committing more expensive thermal units.

The uncertainty of water inflow introduces a relationship between present and future reservoir operation decisions in a cascaded hydro system as shown in Fig. 1. Here, at the optimal point, future and current water values are equal. Water values are calculated as incremental/decremental costs for reducing/adding stored water at the final level in the current period.

The midterm (i.e. several months to 1 year) optimisation of cascaded hydro units is a difficult task because a reservoir's operation strategy may affect downstream reservoirs' energy production and water quantity. In addition, large dimensions, temporal and stochastic characteristics of cascaded hydro systems would require fairly accurate solutions with reasonably low computation costs. In [2, 3], the storage capacity of cascaded reservoirs in a system was aggregated into a single composite reservoir that reduced the number of state variables for long-term studies. The storage and release policies for each reservoir were then disaggregated using heuristic rules. The main drawback of the single composite reservoir model lies in the difficulty to derive feasible/optimal operation policies for individual reservoirs from the aggregate policy. Yu *et al.* [4] proposed a linear marginal cost model to optimise the long-term hydro unit scheduling, which was derived from the composite marginal cost function of a thermal system. The difficulty would be to derive the composite thermal cost function, especially when

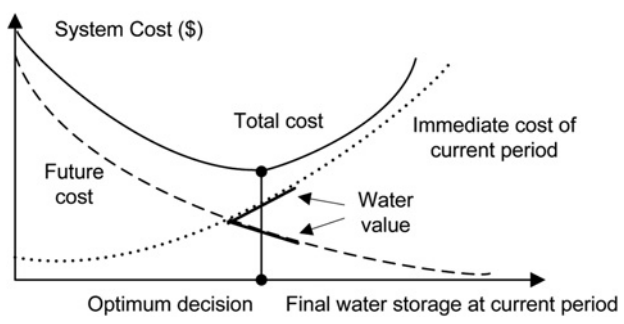

Fig. 1 *Immediate and future costs against final water storage*

incorporating the power transmission network. An overview of the state-of-the-art optimal operation of cascaded reservoir systems was given in [5].

The gas transmission system may affect the operation of power systems with gas-fired generation units. Pressure losses, pipeline contingencies, lack of storage or gas supply disruptions may lead to forced outages of multiple gas-fired units or generation deration. Such events could dramatically increase the power system operating costs and transmission congestion and jeopardise its security [6]. The scheduling of gas-fired combined cycle units could represent a complicated optimisation problem because such units could have multiple operating configurations based on the number and the status of combustion and steam turbines. Lu and Shahidehpour [7] presented an optimisation method for establishing the state space diagram of combined cycle units and applying dynamic programming and Lagrangian relaxation to the security-constrained short-term scheduling of power systems with gas-fired combined cycle units. Non-linear optimisation models for the integrated operation of gas and power systems were discussed in [8, 9]. The impact of gas transmission charges on power markets was discussed in [10]. Li and Shahidehpour [11] proposed an integrated model for assessing the impact of interdependency of electricity and gas networks on power system security. The gas network is modelled by considering daily and hourly limits on pipelines, sub-areas, plants and generating units. Liu *et al.* [12] proposed an integrated model for unit commitment (UC) with gas transmission constraints, which were formulated as non-linear equations and solved by a Newton–Raphson method. Successive benders decomposition (BD) was applied to separate the gas transmission feasibility check subproblem from UC problem. The same methodology is applied here to incorporate gas network constraints into the power system optimal operation problem.

The midterm water allocation could impact the reliability of power systems. Staschus *et al.* [13] modelled hydro unit production using two different methods, that is, through peak shaving or by dispatching hydro units against the equivalent load duration curve (ELDC). It concluded that the ELDC-based approach would generally result in lower production costs and higher reliability by applying hydro units to cover thermal unit outages. Wu *et al.* [14] incorporated reliability into a UC framework by developing loss-of-load-expectation (LOLE) and expected-energy-not-served that provided useful information on long-term operating decisions. Additional details on reliability evaluation methods were given in [15].

In this paper, the reliability assessment of power systems is analysed for the midterm optimal water and gas usages. Since the midterm operation of cascaded reservoirs is coupled in time and space, there is a trade-off between operating cost and supply reliability. Because it is impossible to have prior knowledge of future water inflows, power and gas loads, as well as power system disturbances, this trade-off can only be expressed on a stochastic basis. Uncertainties are simulated by the Monte Carlo (MC) method and a scenario-based technique is applied to keep the trade-off between computation time and accuracy. The stochastic security-constrained unit commitment (SCUC) is used in which the scheduling horizon is decoupled into periodic stages (i.e. several weeks to 1 month) [16]. The periodic operation policy would determine, at the beginning of each period, how much water should be used or stored for the future use. The predefined operation rules are adopted to approximate the actual depletion policy of reservoirs located in a catchment, which would simplify the coupling

doi: 10.1049/iet-gtd.2010.0215

constraints among successive periods and take advantage of the decomposition procedure. The problem is formulated as a two-stage stochastic programming model for the optimisation period of 1 year, with the first stage optimising the operation for the first month and the second stage for the remaining 11 months for simulating the midterm operation via scenarios. In this paper, SCUC would satisfy the hourly electricity and gas network constraints in the base case and all simulated scenarios. Reliability-based solution derived from the proposed two-stage model satisfies the hourly electricity and gas network security constraints and provides sufficient water and gas supply for minimising the load shedding in the entire midterm horizon. Midterm period refers to the scheduling horizon of several months to 1 year, short term refers to several hours to several weeks and long term covers several years.

The rest of the paper is organised as follows. Section 2 presents the solution methodology of the stochastic model. Section 3 presents and discusses a 6-bus system and a modified IEEE 118-bus system, and the conclusion is drawn in Section 4.

2 Stochastic midterm model

The proposed stochastic optimisation problem for analysing the power system reliability and improving the operational efficiency of water and gas usages in a midterm horizon is formulated as a two-stage stochastic model. The objective, formulated in (1), is to minimise the social cost including operation cost (i.e. production cost, startup and shutdown costs of individual units) and the possible load-shedding cost for the entire midterm horizon.

$$\min \sum_{p=1}^{\mathrm{NPD}} \sum_{t=1}^{\mathrm{NT}} \left\{ \begin{array}{l} \sum_{i=1}^{\mathrm{NG}} [F_c(P_{itp}) \cdot I_{itp} + \mathrm{SU}_{itp} + \mathrm{SD}_{itp}] \\ + \sum_{h=1}^{\mathrm{NH}} \mathrm{SU}_{htp} + \sum_{b=1}^{\mathrm{NB}} \sum_{m=1}^{\mathrm{NM}_b} pv_{b,m} \cdot \mathrm{LS}_{btp,m} \end{array} \right\}$$
$$+ \sum_{s=1}^{\mathrm{NS}} p^s \cdot \sum_{p=1+\mathrm{NPD}}^{\mathrm{NPS}+\mathrm{NPD}} \sum_{t=1}^{\mathrm{NT}} \left\{ \begin{array}{l} \sum_{i=1}^{\mathrm{NG}} [F_c(P^s_{itp}) \cdot I^s_{itp} + \mathrm{SU}^s_{itp} + \mathrm{SD}^s_{itp}] \\ + \sum_{h=1}^{\mathrm{NH}} \mathrm{SU}^s_{htp} + \sum_{b=1}^{\mathrm{NB}} \sum_{m=1}^{\mathrm{NM}_b} pv^s_{b,m} \cdot \mathrm{LS}^s_{btp,m} \end{array} \right\} \quad (1)$$

The concept of utilising scenarios adds another dimension to the solution that is different from that of the deterministic midterm UC planning model. The set of constraints includes:

- System power balance constraint.
- Individual generator constraints for various types of units, including ramping up/down rate limits, minimum on/off time limits, generation unit capacity limits etc.
- Individual cascaded hydro unit constraints, including reserve volume limits, water balance constraint, water discharge limits etc. We set the initial and the terminal volumes to be the same in a 1 year horizon to avoid excessive water usage. For the midterm hydro operation, the water usage in the current month is coordinated with that of future months in order to avoid excessive water use in the current month that could lead to the lack of sufficient water supply in future months.
- Power transmission constraints including dc network constraints and phase shifter angles limits.
- Natural gas transmission constraints including gas contract limits, gas usage limits, pipeline and compressor transmission capability limits etc.
- Reliability constraints including load-shedding limits at each bus and each time period in each scenario, and LOLE limits.
- Reservoir volume coupling constraints for two consecutive periods, which indicates that the terminal volume at the end of previous period should be the initial volume at the beginning of successive period.

Detailed formulations of constraints for the system and individual generators are found in [16], cascaded hydro system formulation in [17], reliability formulation in [14] and gas network formulation in [12]. The contributions of this paper reside in the formulation of midterm hydro reservoir operation, the optimisation and the coordination of midterm water and natural gas usage, and the proposed solution methodology for the complex midterm scheduling problem by fully utilising the capabilities of state-of-the-art mixed-integer programming, Lagrangian relaxation and BD techniques.

2.1 Scenario techniques with MC

A set of scenarios is generated by MC for simulating power system uncertainties, including random outages of system components, electric and gas load forecast errors and uncertainties associated with water inflows. The advantage of applying MC is that the simulation accuracy of MC depends on the number of samples rather than the dimension of uncertainty in each scenario. Therefore MC is suitable for power systems with large dimensions of uncertainty.

A two-state continuous-time Markov chain model is applied to simulate component outages in each scenario and UC states are calculated by solving the stochastic SCUC problem. The parameters used for MC are failure and repair rates of each power system component. The water inflow to a reservoir follows a discrete Markov chain, which is independent of inflows to other reservoirs, thus the spatially independent log-normal random variable correlated in time with a first-order lag is used to simulate the water inflow. The detailed formulations are provided in [16, 17]. The future power load and gas load uncertainty is represented by a truncated normal distribution with a probability density function shown in (2). The distribution is divided into a discrete number of intervals (i.e. μ, $\mu \pm \sigma$, $\mu \pm 2\sigma$, $\mu \pm 3\sigma$ etc) and the load in the mid-point of each interval represents the probability of the interval, where μ is the forecasted load and σ is the known standard deviation.

The Latin hypercube sampling is developed to generate multi-dimensional random numbers to compose a set of scenarios. The scenario reduction can reduce the computational time by eliminating scenarios with very low probabilities and bundling scenarios that are very close in terms of statistical metrics [16–18].

$$f(x) = \begin{cases} 0 & x < \mu - 3.5\sigma \text{ or } x > \mu + 3.5\sigma \\ \dfrac{1}{\alpha\sqrt{2\pi}\sigma} \cdot \mathrm{e}^{-((x-\mu)^2/2\sigma^2)} & \mu - 3.5\sigma \le x \le \mu + 3.5\sigma \end{cases}$$
$$\text{where } \alpha = \int_{\mu-3.5\sigma}^{\mu+3.5\sigma} \frac{1}{\sqrt{2\pi}\sigma} \cdot \mathrm{e}^{-((x-\mu)^2/2\sigma^2)} \mathrm{d}x \quad (2)$$

2.2 Midterm reservoir operation rules

Simplified operation rules that approximate the depletion policy of cascaded reservoirs may be used to estimate the energy production [19]. The adopted operation rules define the volume of each reservoir V_h in a catchment as a function of γ_c corresponding to catchment c. That is, a set of curves is adopted for describing the relationship between the global parameter (one global parameter per catchment) and each reservoir volume in the catchment as

$$V_h = \Psi(\gamma_c) \quad \forall h \in c \tag{3}$$

The operation rule is given based on historical inflow records or non-linear optimisation model [20]. As shown in Fig. 2, the operation rule does not have to represent a convex curve.

The following two formulations can be applied for mixed-integer linear programming (MIP) modelling of non-convex operation rule curves. Numbers of integer variables and constraints are often regarded as good indicators of computational difficulty of MIP models [21]. Considering a NV_h segments curve shown in Fig. 2, Formulation 1 is based on the type 1 special ordered set (SOS1), which forms variables within which only one is non-zero and would facilitate the branching process of branch-and-bound method for a faster convergence [21, 22]. Different from Formulation 1 which introduces integer variables corresponding to each of NV_h segments, Formulation 2 includes integer variables corresponding to each of $\mathrm{NV}_h - 1$ intermediate points, thus containing less integer variables than Formulation 1. The number of variables and constraints are listed in Table 1 for comparison. Although Formulation 1 introduces one more integer variable than Formulation 2, there would be NV_h nodes in either case by the branch-and-bound tree in the worst case. An MIP model is often easier to solve by expanding a limited number of constraints, which provides a tighter approximated MIP formulation and will be used in the tree search strategy. Based on our experience with different formulations for large systems, Formulation 2 is tighter and converges faster and used in this paper.

Formulation 1

$$V_h = V_{h,\min} \cdot \delta_{h,1} + \sum_{m=2}^{\mathrm{NV}_h} V_{h,m-1} \cdot \delta_{h,m} + \sum_{m=1}^{\mathrm{NV}_h} \mathrm{IC}_{h,m} \cdot v_{h,m}$$

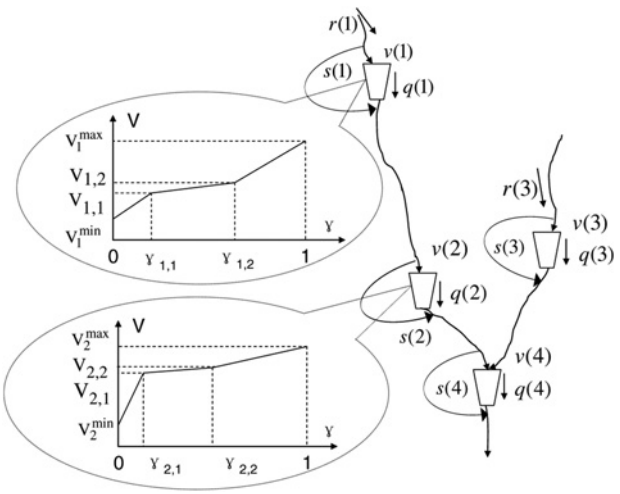

Fig. 2 *Depletion curves for a catchment*

Table 1 Comparison of MIP formulations

	Formulation 1	Formulation 2
number of integer variables	NV_h	$\mathrm{NV}_h - 1$
number of total variables	$2 \cdot \mathrm{NV}_h + 2$	$2 \cdot \mathrm{NV}_h + 1$
number of equality constraints	3	2
number of inequality constraints (limits of variables do not count in)	NV_h	$2 \cdot \mathrm{NV}_h - 2$

$$\begin{aligned}
&\gamma_c = 0 \cdot \delta_{h,1} + \sum_{m=2}^{\mathrm{NV}_h} \gamma_{h,m-1} \cdot \delta_{h,m} + \sum_{m=1}^{\mathrm{NV}_h} v_{h,m} \\
&\sum_{m=1}^{\mathrm{NV}_h} \delta_{h,m} = 1 \quad \delta_{h,m} \in \{0, 1\} \\
&0 \le v_{h,1} \le (\gamma_{h,1} - 0) \cdot \delta_{h,1} \\
&0 \le v_{h,m} \le (\gamma_{h,m} - \gamma_{h,m-1}) \cdot \delta_{h,m} m \in \{2, \ldots, \mathrm{NV}_h - 1\} \\
&0 \le v_{h,\mathrm{NV}_h} \le (1 - \gamma_{h,\mathrm{NV}_h - 1}) \cdot \delta_{h,\mathrm{NV}_h}
\end{aligned} \tag{4}$$

Formulation 2

$$\begin{aligned}
&V_h = V_{h,\min} + \sum_{m=1}^{\mathrm{NV}_h} \mathrm{IC}_{h,m} \cdot v_{h,m} \\
&\gamma_c = 0 + \sum_{m=1}^{\mathrm{NV}_h} v_{h,m} \\
&(\gamma_{h,1} - 0) \cdot \delta_{h,1} \le v_{h,1} \le (\gamma_{h,1} - 0) \\
&(\gamma_{h,m} - \gamma_{h,m-1}) \cdot \delta_{h,m} \le v_{h,m} \le (\gamma_{h,m} - \gamma_{h,m-1}) \cdot \delta_{h,m-1} \\
&m \in [2, \mathrm{NV}_h - 1] \\
&0 \le v_{h,\mathrm{NV}_h} \le (1 - \gamma_{h,\mathrm{NV}_h - 1}) \cdot \delta_{h,\mathrm{NV}_h - 1} \\
&\delta_{h,m} \in \{0, 1\}
\end{aligned} \tag{5}$$

2.3 Proposed stochastic solution

Scenarios add another dimension to the proposed solution of midterm model, which makes the proposed two-stage stochastic problem very large and computationally impractical. A proper decomposition procedure is necessary for decomposing the problem into tractable easy-to-solve subproblems for each period.

In order to consider midterm optimal water usage, reservoir volume coupling constraints between consecutive periods would need to be considered, which states that the terminal volume of one period would be the same as the initial volume of the next period. Thus, the midterm horizon is divided into several periods, with the relaxation of reservoir volume coupling limits for linking successive periods. Other coupling constraints, such as ramping up/down rate limits, minimum on/off time constraints and delayed water discharge from upper reservoirs to lowers, which link successive periods, are managed based on one of the following two strategies:

1. Constraints linking successive periods will be ignored. Accordingly, the short-term UC problem can be solved for each period independently. The application of parallel

doi: 10.1049/iet-gtd.2010.0215

processing will speed up the solution. However, the accuracy may suffer slightly.

2. Short-term UC subproblems are solved sequentially. That is, the results of the short-term UC for the first period provide initial conditions for the second period. In this case, constraints linking successive periods will be satisfied within each period by UC.

The difference between the two alternatives signifies the trade-off between speed and accuracy. In this paper, we adopt the second alternative. The reservoir volume which links successive periods is relaxed by introducing artificially duplicated variables of common variables in (6). In (6), the first and third constraints correspond to the reservoir volume coupling constraint between successive periods at the first and second stages, respectively, and the second constraint is for the coupling constraint between the last period of the first stage and the first period of the second stage. Based on the midterm reservoir operation rule discussed earlier, (6) is substituted by (7) by using γ_c for each catchment c.

The introduction of global parameter γ_c, which uniformly adjusts reservoir volumes in a catchment, reduces the number of coupling constraints that are to be relaxed from $\mathrm{NH}\cdot[(\mathrm{NPD}-1)+\mathrm{NS}+\mathrm{NS}\cdot(\mathrm{NPS}-1)]$ in (6) to $\mathrm{NC}\cdot[(\mathrm{NPD}-1)+\mathrm{NS}+\mathrm{NS}\cdot(\mathrm{NPS}-1)]$ in (7). By introducing a set of Lagrangian multipliers, coupling constraints (7) are relaxed and the Lagrangian dual function of the original problem (1) is formulated as (8). Equation (8) can be easily separated into tractable subproblems, (9)–(11), corresponding to periods at the first stage and (12)–(14) corresponding to periods of each scenario at the second stage. A decomposition approach is used for solving each subproblem with respect to constraints discussed at the beginning of Section 2.

$$\begin{aligned}
&V_{h\mathrm{NT}p}=V_{h0(p+1)} \quad \forall h,\ \forall p\in\{1,\ \ldots,\ \mathrm{NPD}-1\}\\
&V_{h\mathrm{NT}p}=V^s_{h0(p+1)} \quad \forall s,\ \forall h,\ p=\mathrm{NPD}\\
&V^s_{h\mathrm{NT}p}=V^s_{h0(p+1)} \quad \forall s,\ \forall h,\ \forall p\in\left\{\begin{matrix}\mathrm{NPD}+1,\ \ldots,\\ \mathrm{NPD}+\mathrm{NPS}-1\end{matrix}\right\}
\end{aligned} \tag{6}$$

$$\begin{aligned}
&\gamma_{c\mathrm{NT}p}=\gamma_{c0(p+1)} \quad \forall c,\ \forall p\in\{1,\ \ldots,\ \mathrm{NPD}-1\}\\
&\gamma_{c\mathrm{NT}p}=\gamma^s_{c0(p+1)} \quad \forall s,\ \forall c,\ p=\mathrm{NPD}\\
&\gamma^s_{c\mathrm{NT}p}=\gamma^s_{c0(p+1)} \quad \forall s,\ \forall c,\ \forall p\in\left\{\begin{matrix}\mathrm{NPD}+1,\ \ldots,\\ \mathrm{NPD}+\mathrm{NPS}-1\end{matrix}\right\}
\end{aligned} \tag{7}$$

$$\begin{aligned}
L(\beta)=\min\sum_{p=1}^{\mathrm{NPD}}\sum_{t=1}^{\mathrm{NT}}\Bigg\{&\sum_{i=1}^{\mathrm{NG}}[F_c(P_{itp})\cdot I_{itp}+\mathrm{SU}_{itp}+\mathrm{SD}_{itp}]\\
&+\sum_{h=1}^{\mathrm{NH}}\mathrm{SU}_{htp}+\sum_{b=1}^{\mathrm{NB}}\sum_{m=1}^{\mathrm{NM}_b}pv_{b,m}\cdot\mathrm{LS}_{btp,m}\Bigg\}\\
&+\sum_{s=1}^{\mathrm{NS}}p^s\cdot\sum_{p=1+\mathrm{NPD}}^{\mathrm{NPS}+\mathrm{NPD}}\sum_{t=1}^{\mathrm{NT}}\Bigg\{\sum_{i=1}^{\mathrm{NG}}[F_c(P^s_{itp})\cdot I^s_{itp}\\
&+\mathrm{SU}^s_{itp}+\mathrm{SD}^s_{itp}]+\sum_{h=1}^{\mathrm{NH}}\mathrm{SU}^s_{htp}\\
&+\sum_{b=1}^{\mathrm{NB}}\sum_{m=1}^{\mathrm{NM}_b}pv^s_{b,m}\cdot\mathrm{LS}^s_{btp,m}\Bigg\}
\end{aligned}$$

$$\begin{aligned}
&+\sum_{c=1}^{\mathrm{NC}}\left\{\begin{matrix}\sum_{p=1}^{\mathrm{NPD}-1}\beta_{cp}\cdot(\gamma_{c\mathrm{NT}p}-\gamma_{c0(p+1)})\\ +\sum_{s=1}^{\mathrm{NS}}\beta^s_c\cdot(\gamma_{c\mathrm{NTNPD}}-\gamma^s_{c0(\mathrm{NPD}+1)})\\ +\sum_{s=1}^{\mathrm{NS}}\sum_{p=1+\mathrm{NPD}}^{\mathrm{NPS}+\mathrm{NPD}-1}\beta^s_{cp}\cdot(\gamma^s_{c\mathrm{NT}p}-\gamma^s_{c0(p+1)})\end{matrix}\right\} \qquad (8)\\
&\min\sum_{t=1}^{\mathrm{NT}}\left\{\begin{matrix}\sum_{i=1}^{\mathrm{NG}}[F_c(P_{it1})\cdot I_{it1}+\mathrm{SU}_{it1}+\mathrm{SD}_{it1}]\\ +\sum_{h=1}^{\mathrm{NH}}\mathrm{SU}_{ht1}+\sum_{b=1}^{\mathrm{NB}}\sum_{m=1}^{\mathrm{NM}_b}pv_{b,m}\cdot\mathrm{LS}_{bt1,m}\end{matrix}\right\}\\
&\quad+\sum_{c=1}^{\mathrm{NC}}\beta_{c1}\cdot\gamma_{c\mathrm{NT}1} \qquad (9)\\
&\min\sum_{t=1}^{\mathrm{NT}}\left\{\begin{matrix}\sum_{i=1}^{\mathrm{NG}}[F_c(P_{itp})\cdot I_{itp}+\mathrm{SU}_{itp}+\mathrm{SD}_{itp}]\\ +\sum_{h=1}^{\mathrm{NH}}\mathrm{SU}_{htp}+\sum_{b=1}^{\mathrm{NB}}\sum_{m=1}^{\mathrm{NM}_b}pv_{b,m}\cdot\mathrm{LS}_{btp,m}\end{matrix}\right\}\\
&\quad+\sum_{c=1}^{\mathrm{NC}}\{\beta_{cp}\cdot\gamma_{c\mathrm{NT}p}-\beta_{c(p-1)}\cdot\gamma_{c0p}\} \qquad (10)\\
&\quad\forall p\in\{2,\ \ldots,\ \mathrm{NPD}-1\}
\end{aligned}$$

The approach applies BD for separating UC in the master problem from the dc network and the gas network security check in subproblems. Successive linear programming is applied to solve the gas transmission feasibility check. If any electric power network or gas network violations arise, corresponding Benders cuts are formed and added to the master problem for solving the next iteration [12].

$$\begin{aligned}
&\min\sum_{t=1}^{\mathrm{NT}}\left\{\begin{matrix}\sum_{i=1}^{\mathrm{NG}}[F_c(P_{itp})\cdot I_{itp}+\mathrm{SU}_{itp}+\mathrm{SD}_{itp}]\\ +\sum_{h=1}^{\mathrm{NH}}\mathrm{SU}_{htp}+\sum_{b=1}^{\mathrm{NB}}\sum_{m=1}^{\mathrm{NM}_b}pv_{b,m}\cdot\mathrm{LS}_{btp,m}\end{matrix}\right\}\\
&\quad+\sum_{c=1}^{\mathrm{NC}}\left\{\sum_{s=1}^{\mathrm{NS}}\beta^s_c\cdot\gamma_{c\mathrm{NT}p}-\beta_{c(p-1)}\cdot\gamma_{c0p}\right\}\quad p=\mathrm{NPD} \qquad (11)\\
&\min p^s\cdot\sum_{t=1}^{\mathrm{NT}}\left\{\begin{matrix}\sum_{i=1}^{\mathrm{NG}}[F_c(P^s_{itp})\cdot I^s_{itp}+\mathrm{SU}^s_{itp}+\mathrm{SD}^s_{itp}]\\ +\sum_{h=1}^{\mathrm{NH}}\mathrm{SU}^s_{htp}+\sum_{b=1}^{\mathrm{NB}}\sum_{m=1}^{\mathrm{NM}_b}pv^s_{b,m}\cdot\mathrm{LS}^s_{btp,m}\end{matrix}\right\}\\
&\quad+\sum_{c=1}^{\mathrm{NC}}\{\beta^s_{cp}\cdot\gamma^s_{c\mathrm{NT}p}-\beta^s_c\cdot\gamma^s_{c0p}\}\quad p=\mathrm{NPD}+1 \qquad (12)\\
&\min p^s\cdot\sum_{t=1}^{\mathrm{NT}}\left\{\begin{matrix}\sum_{i=1}^{\mathrm{NG}}[F_c(P^s_{it1})\cdot I^s_{it1}+\mathrm{SU}^s_{it1}+\mathrm{SD}^s_{it1}]\\ +\sum_{h=1}^{\mathrm{NH}}\mathrm{SU}^s_{ht1}+\sum_{b=1}^{\mathrm{NB}}\sum_{m=1}^{\mathrm{NM}_b}pv^s_{b,m}\cdot\mathrm{LS}^s_{bt1,m}\end{matrix}\right\}\\
&\quad+\sum_{c=1}^{\mathrm{NC}}\{\beta^s_{cp}\cdot\gamma^s_{c\mathrm{NT}p}-\beta^s_{c(p-1)}\cdot\gamma^s_{c0p}\} \qquad (13)\\
&\quad\forall p\in\{\mathrm{NPD}+2,\ \ldots,\ \mathrm{NPD}+\mathrm{NPS}-1\}
\end{aligned}$$

$$\min p^s \cdot \sum_{t=1}^{\mathrm{NT}} \left\{ \begin{array}{l} \sum_{i=1}^{\mathrm{NG}} [F_c(P^s_{itp}) \cdot I^s_{itp} + \mathrm{SU}^s_{itp} + \mathrm{SD}^s_{itp}] \\ + \sum_{h=1}^{\mathrm{NH}} \mathrm{SU}^s_{htp} + \sum_{b=1}^{\mathrm{NB}} \sum_{m=1}^{\mathrm{NM}_b} pv^s_{b,m} \cdot \mathrm{LS}^s_{btp,m} \end{array} \right\} - \sum_{c=1}^{\mathrm{NC}} \beta^s_{c(p-1)} \cdot \gamma^s_{c0p} \quad p = \mathrm{NPD} + \mathrm{NPS} \tag{14}$$

Since Lagrangian dual function is non-differentiable, the standard subgradient method would result in a slow convergence. A proximal Bundle method is used, which diminishes the unstable behaviour of cutting-plane algorithm and speeds up the convergence process by adding the trust region philosophy [23, 24].

First $\overline{\beta} = \{\overline{\beta}_{cp}, \overline{\beta}^s_c, \overline{\beta}^s_{cp}\}$ is selected among the current set of available solutions, which is typically the one that provides the largest $L(\beta)$. The quadratic problem (15) is solved to find $\beta^k = \{\beta^k_{cp}, \beta^{k,s}_c, \beta^{k,s}_{cp}\}$ for the next iteration, where Δ^j is the linearisation error. Here, $\|\cdot\|$ is the Euclidean norm and α^k is an iteration-variant positive parameter, called the trust-region parameter, which decides the region that can be trusted as an approximation for $L(\beta)$.

Several issues are discussed here for an efficient bundle algorithm, including the dynamic choice of parameter α^k, updating strategy for the current point $\overline{\beta}$ and stopping criterion. At each iteration, k, the current point $\overline{\beta}$ will be shifted to β^k only if (16) is satisfied and α^k for the next iteration will be increased to enlarge the trust region if (17) is not satisfied.

Otherwise, the current solution of iteration k is added to the bundle if Δ^k is small compared to a predefined threshold. If the condition is not satisfied, we discard the solution of this iteration and reduce α^k to shrink the trust region for solving (15) again. The α^k updating strategy is as follows:

- Predefine lower and upper bounds of α, $\alpha\mathrm{Min}$ and $\alpha\mathrm{Max}$ as $\alpha^0 = (\alpha^0_{\mathrm{Min}} + \alpha^0_{\mathrm{Max}})/2$, $\alpha^0_{\mathrm{Min}} = \alpha\mathrm{Min}$, $\alpha^0_{\mathrm{Max}} = \alpha\mathrm{Max}$.
- For each iteration k, set $\alpha^k_{\mathrm{Min}} = \alpha^{k-1}$ if α^k is to be increased; otherwise set $\alpha^k_{\mathrm{Max}} = \alpha^{k-1}$ and the new α^k will be calculated as $\alpha^k = (\alpha^k_{\mathrm{Min}} + \alpha^k_{\mathrm{Max}})/2$.

$$\max_{\beta^k_{cp}, \beta^{k,s}_c, \beta^{k,s}_{cp}} \left\{ \mathrm{EV}^k - \frac{1}{2 \cdot \alpha^k} \|\beta^k - \overline{\beta}\|^2 \right\}$$

s.t.

$$EV^k \le \Delta^j + \sum_{c=1}^{\mathrm{NC}} \left\{ \begin{array}{l} \sum_{p=1}^{\mathrm{NPD}-1} (\beta_{cp} - \overline{\beta}_{cp}) \cdot (\gamma^j_{c\mathrm{NT}p} - \gamma^j_{c0(p+1)}) \\ + \sum_{s=1}^{\mathrm{NS}} (\beta^s_c - \overline{\beta}^s_c) \cdot (\gamma^j_{c\mathrm{NTNPD}} - \gamma^{j,s}_{c0(\mathrm{NPD}+1)}) \\ + \sum_{s=1}^{\mathrm{NS}} \sum_{p=1+\mathrm{NPD}}^{\mathrm{NPS}+\mathrm{NPD}-1} (\beta^s_{cp} - \overline{\beta}^s_{cp}) \cdot (\gamma^{j,s}_{c\mathrm{NT}p} - \gamma^{j,s}_{c0(p+1)}) \end{array} \right\} \tag{15}$$

$$\Delta^j = L(\beta^j) - L(\overline{\beta}) + \sum_{c=1}^{\mathrm{NC}} \left\{ \begin{array}{l} \sum_{p=1}^{\mathrm{NPD}-1} (\overline{\beta}_{cp} - \beta^j_{cp}) \cdot (\gamma^j_{c\mathrm{NT}p} - \gamma^j_{c0(p+1)}) \\ + \sum_{s=1}^{\mathrm{NS}} (\overline{\beta}^s_c - \beta^{j,s}_c) \cdot (\gamma^j_{c\mathrm{NTNPD}} - \gamma^{j,s}_{c0(\mathrm{NPD}+1)}) \\ + \sum_{s=1}^{\mathrm{NS}} \sum_{p=1+\mathrm{NPD}}^{\mathrm{NPS}+\mathrm{NPD}-1} (\overline{\beta}^s_{cp} - \beta^{j,s}_{cp}) \cdot (\gamma^{j,s}_{c\mathrm{NT}p} - \gamma^{j,s}_{c0(p+1)}) \end{array} \right\}$$

$$[L(\beta^k) - L(\overline{\beta})]/L(\overline{\beta}) \ge \varepsilon_1 \tag{16}$$

$$\sum_{c=1}^{\mathrm{NC}} \left\{ \begin{array}{l} \sum_{p=1}^{\mathrm{NPD}-1} (\beta^k_{cp} - \overline{\beta}_{cp}) \cdot (\gamma^k_{c\mathrm{NT}p} - \gamma^k_{c0(p+1)}) \\ + \sum_{s=1}^{\mathrm{NS}} (\beta^{k,s}_c - \overline{\beta}^s_c) \cdot (\gamma^k_{c\mathrm{NTNPD}} - \gamma^{k,s}_{c0(1+\mathrm{NPD})}) \\ + \sum_{s=1}^{\mathrm{NS}} \sum_{p=1+\mathrm{NPD}}^{\mathrm{NPS}+\mathrm{NPD}-1} (\beta^{k,s}_{cp} - \overline{\beta}^s_{cp}) \cdot (\gamma^{k,s}_{c\mathrm{NT}p} - \gamma^{k,s}_{c0(p+1)}) \end{array} \right\} \le \varepsilon_2 \tag{17}$$

The process stops when the Lagrangian multiplier difference between two successive iterations is smaller than the predefined threshold ε_3 in (18). The solution that satisfies the stopping criterion may not satisfy the relaxed constraints (6)–(7). Equation (19) calculates the degree of violation of relaxed constraints (6)–(7). A feasible solution is constructed by heuristically adjusting the initial and terminal reservoir volumes at each period based on the system load at successive periods (20)–(22), which are calculated and used as limits for the problem optimisation at the final run. Because ΔV is small when the stopping criterion is met, and reservoirs have spillage capability, the final run will not encounter infeasibility by minor adjustments of reservoir volumes (20)–(22).

$$\|\beta^k - \overline{\beta}\|^2 = \sum_{c=1}^{\mathrm{NC}} \left\{ \sum_{p=1}^{\mathrm{NPD}-1} (\beta^k_{cp} - \overline{\beta}_{cp})^2 + \sum_{s=1}^{\mathrm{NS}} (\beta^{k,s}_c - \overline{\beta}^s_c)^2 + \sum_{s=1}^{\mathrm{NS}} \sum_{p=1+\mathrm{NPD}}^{\mathrm{NPS}+\mathrm{NPD}-1} (\beta^{k,s}_{cp} - \overline{\beta}^s_{cp})^2 \right\} \le \varepsilon_3 \tag{18}$$

$$\Delta V = \sqrt{\sum_{h=1}^{\mathrm{NH}} \left\{ \begin{array}{l} \sum_{p=1}^{\mathrm{NPD}-1} (V_{h\mathrm{NT}p} - V_{h0(p+1)})^2 \\ + \sum_{s=1}^{\mathrm{NS}} (V_{h\mathrm{NTNPD}} - V^s_{h0(1+\mathrm{NPD})})^2 \\ + \sum_{s=1}^{\mathrm{NS}} \sum_{p=1+\mathrm{NPD}}^{\mathrm{NPS}+\mathrm{NPD}-1} (V^s_{h\mathrm{NT}p} - V^s_{h0(p+1)})^2 \end{array} \right\}} \tag{19}$$

$$V^F_{h\mathrm{NT}p} = V^F_{h0(p+1)} = V^k_{h\mathrm{NT}p} + (V^k_{h0(p+1)} - V^k_{h\mathrm{NT}p}) \cdot \frac{\sum_t \mathrm{PL}_{tp}}{\sum_t \mathrm{PL}_{tp} + \sum_t \mathrm{PL}_{t(p+1)}} \quad \forall p \in \{1, \ldots, \mathrm{NPD}-1\} \tag{20}$$

doi: 10.1049/iet-gtd.2010.0215

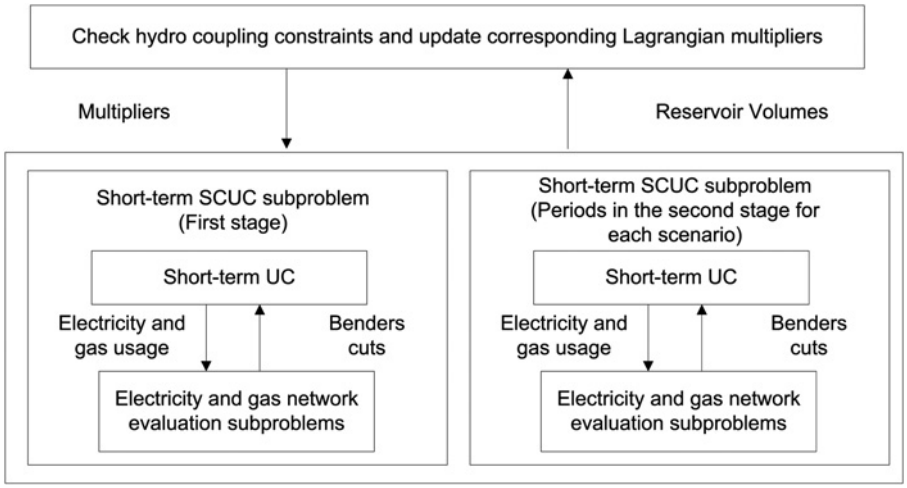

Fig. 3 *Optimisation and coordination for the midterm operation planning with optimal usage for water and natural gas*

$$V^{F}_{h\mathrm{NT}p} = V^{F}_{h0(p+1)} = V^{k}_{h\mathrm{NT}p} + \left(\sum_{s} p^{s} \cdot V^{k,s}_{h0(p+1)} - V^{k}_{h\mathrm{NT}p}\right) \cdot \frac{\sum_{t} \mathrm{PL}_{tp}}{\sum_{t} \mathrm{PL}_{tp} + \sum_{s} p^{s} \cdot \left(\sum_{t} \mathrm{PL}^{s}_{t(p+1)}\right)} \quad p = \mathrm{NPD} \tag{21}$$

$$V^{F,s}_{h\mathrm{NT}p} = V^{F,s}_{h0(p+1)} = V^{k,s}_{h\mathrm{NT}p} + (V^{k,s}_{h0(p+1)} - V^{k,s}_{h\mathrm{NT}p}) \cdot \frac{\sum_{t} \mathrm{PL}^{s}_{tp}}{\sum_{t} \mathrm{PL}^{s}_{tp} + \sum_{t} \mathrm{PL}^{s}_{t(p+1)}} \quad \forall p \in \left\{ \begin{array}{c} \mathrm{NPD}+1, \ldots, \\ \mathrm{NPD}+\mathrm{NPS}-1 \end{array} \right\} \tag{22}$$

Fig. 3 shows the solution strategy for decomposing the large-scale problem into tractable easy-to-solve subproblems. With the relaxation of reservoir volume coupling constraints by introducing Lagrangian multipliers, the midterm problem is divided into several short-term sub-problems, corresponding to the period in the first stage and periods in the second stage for each scenario. For each short-term SCUC sub-problem, BD is applied for separating UC in the master problem from the hourly dc network and gas network evaluation in sub-problems. If any electric power network or gas network violations arise, corresponding Benders cuts are formed and added to the master problem for solving the next iteration [12]. After obtaining the hydro schedules from the short-term operation sub-problems, the coupling constraints of reservoir volume are checked. If the constraints are violated, the corresponding Lagrangian multipliers are updated. The Lagrangian iterations will continue until a near optimal solution is reached, and the final feasible solution is constructed by heuristically adjusting the initial and terminal reservoir volumes at each period.

3 Case study

A 6-bus system and the IEEE 118-bus system are considered to demonstrate the proposed approach for the optimal scheduling of midterm water and gas usages.

3.1 6-bus system

The 6-bus system in Fig. 4 is used to illustrate the proposed method. The system has three gas-fired units, one hydro unit and seven transmission lines. The hydro unit data are shown in Table 2. Other detailed generator, transmission line and gas network data are given in [12]. Failure and repair rates for transmission lines are 0.0671 failures/year and 0.9329 repairs/year.

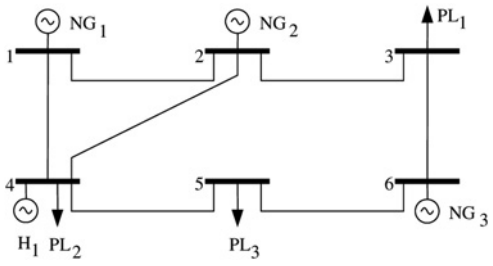

Fig. 4 *One-line diagram of six-bus example*

Table 2 Parameters of hydro unit

efficiency	h0	α	discharge max, $\times 10^4$ m^3	discharge min, $\times 10^4$ m^3
8.091	0.857	0.0001315	10	1
Pmin, MW	Pmax, MW	Ramp, MW/h	min on, h	min off, h
9	80	60	1	1
volume min, $\times 10^4$ m^3	volume max, $\times 10^4$ m^3	initial volume $\times 10^4$ m^3	terminal volume, $\times 10^4$ m^3	initial hour
60	1000	1000	1000	1
		Operation rule		
global parameter	0	0.25	0.75	1
volume, $\times 10^4$ m^3	60	250	800	1000

Failure and repair rates for generating units are listed in Table 3. The system is tested for a one-year case (from November to the following October) with the annual peak power load of 330 MW and annual peak gas load of 6000 kcf. Fig. 5 shows the weekly peak loads as a percentage of annual peak load. The maximum allowable load shedding is set to be the load value at the designated bus, with a VOLL of 5000 $/MWh for the first 10% of the load and 2000 $/MWh for the remaining. For the 6-bus system, each period refers to a month. Thus, the first stage contains one period and the second stage contains 11 periods in each scenario.

Two cases are studied to illustrate the effect of midterm water and gas optimal usages on power system reliability:

Case 1: A deterministic solution in the winter season is presented and its impact on the system reliability is discussed, where forced outage rates are assumed to be negligible and the power and gas loads given in Fig. 5 are used. The uncertainty of water inflow is not considered, and thus the terminal reservoir volume is not restricted. The optimisation of deterministic model utilises as much water as possible to supplement the gas usage in the winter season (November–January with highest gas loads). The impact of the deterministic solution on the system reliability is considered by optimising a scenario-based stochastic model for the remaining months of February–October by utilising terminal volumes at the end of January as the initial condition.

The computation time for the scenario-based problem depends on the number of scenarios. The scenario reduction method would reduce the total number of scenarios from 100 to 12 as a trade-off between calculation speed and solution accuracy. Table 4 shows the weights of each scenario after reduction. The results of the first 3 months in Case 1 are presented in Table 5.

Table 3 Failure and repair rates of generators

Units	NG1	NG2	NG3	H1
failure rate, failures/year	0.0307	0.0286	0.0259	0.0262
repair rate, repairs/year	2.4444	2.2749	2.0622	2.0893

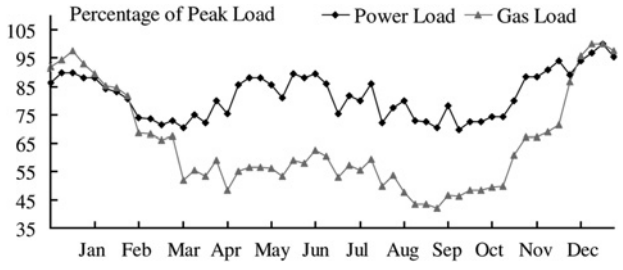

Fig. 5 *Weekly peak loads as a percentage of annually peak load*

Table 4 Weights of each scenario after scenario reduction

Scenario	1	2	3	4	5	6
weight	0.07	0.075	0.18	0.035	0.065	0.24
Scenario	7	8	9	10	11	12
weight	0.07	0.045	0.045	0.01	0.04	0.125

Owing to the limited capability of gas network, the gas required by gas-fired generating units cannot be transported to corresponding nodes by the gas transmission system. The water resource is the alternative energy to cover the load. It is shown that most of the water reservoir is used in December because of the highest demand by gas loads shown in Fig. 5. The terminal reservoir volume at the end of winter reaches its minimum value of 60×10^4 m^3 because the terminal reservoir volume is not restricted and the water resource in the reservoir is used as much as possible. We use the terminal volume at the end of winter, as the initial condition for the following seasons, and 1000×10^4 m^3 as the terminal volume for the remaining 9 months. The resulting social cost and load shedding for each scenario is listed in Table 6. Based on results presented in Tables 6 and 7, the social cost is $39 585 164.34 (i.e. 12 141 356.75 + 27 443 807.59) with a load shedding of 460.91 MWh. The annual load shedding is 96.465 h.

Case 2: The proposed two-stage stochastic optimisation model is discussed. The first stage covers the first month and the second stage includes the remaining 11 months via scenarios. The uncertainties of system component availability, power and gas load levels and water inflows are considered. Table 7 shows that by the midterm stochastic optimisation of water and gas usages, one can optimally allocate the water resource to enhance the system reliability. In comparison with Case 1, load shedding is reduced from 460.91 to 440.90 MWh. The annual load shedding is reduced from 96.465 to 71.07 h. The reservoir water, previously utilised fully in Case 1, is now partly allocated to the summer for peak-shaving. The social cost in comparison with Case 1 is reduced by 5.08% (i.e. 39 585 164.34 – 37 572 145.9/39 585 164.34.)

For this Case, the period for the first stage and periods corresponding to each scenario in the second stage are solved sequentially. The CPU time consumed for one

Table 5 Results for the first 3 months in Case 1

social cost, $		12 141 356.75
LS, MWh		411.42
number of hours LS occurs		56
volume at the end of each month, $\times 10^4$ m^3	11	860.34
	12	65.83
	1	60.00

Table 6 Results for the following seasons based on Case 1

Scenario	Social cost, $	LS, MWh	Number of LS hours
1	27 659 311.07	53.62	57
2	27 425 028.63	37.29	35
3	27 678 604.15	53.10	39
4	27 551 233.52	54.52	43
5	27 296 860.88	38.91	47
6	27 672 777.70	43.15	29
7	27 608 847.21	57.60	48
8	28 646 885.12	45.15	40
9	26 587 588.48	43.03	33
10	28 715 483.62	76.87	54
11	27 667 616.62	57.55	50
12	26 212 352.22	60.16	49
expected	27 443 807.59	49.49	40.465

doi: 10.1049/iet-gtd.2010.0215

Table 7 Results for Case 2

First-stage solution			
social cost		3 473 861.69	
LS, MWh		0	
number of LS hours		0	
terminal volume, $\times 10^4$ m^3		984.29	
Second-stage solution			
Scenario	Social cost, $	LS, MWh	Number of LS hours
1	34 234 442.97	426.7466	82
2	33 745 037.61	447.1278	58
3	34 337 516.25	436.0846	63
4	33 707 806.17	426.1430	66
5	33 513 715.31	422.8795	72
6	33 985 407.29	446.8944	64
7	34 046 856.81	452.2434	69
8	35 486 860.11	432.0145	79
9	33 888 175.90	423.6509	71
10	36 731 962.03	444.9300	94
11	33 916 433.81	452.5987	88
12	33 971 571.38	452.9742	90
expected	34 098 284.21	440.9000	71.07

scenario is about 15 min and about 60 h (i.e. no. of scenarios × no. of iterations × 15 min) for the entire two-stage stochastic programming on a 3.2 GHz Pentium 4 personal computer. However, parallel computing applied to scenarios would rapidly reduce the CPU time to 5 h.

Fig. 6 shows the optimal monthly water resource allocations for Case 1 and two scenarios of Case 2, representing a wet and a dry weather. In Case 1, the reservoir water is used fully when the future water inflow situation is not considered. Two scenarios, a dry and a wet year, presented in Fig. 6 show that when the uncertainty of water inflow is considered, the water used in winter would have to be limited in order to cover the summer peaks. Fig. 6 shows that reservoir volumes for wet and dry scenarios are decreased in June since the water is discharged for peak load shaving. That is, the terminal volumes at the end of January are higher than that of Case 1 to cover a possible dry summer season. Fig. 6 shows that for the dry scenario, the water usage in November through January is strictly limited with the limited reservoir refilling. This is because of the less available water resource in January through April. The results reveal the necessity of incorporating a two-stage stochastic optimisation model for the midterm water and gas management to enhance the system reliability.

In order to demonstrate the convergence process, Fig. 7 presents the iterative Lagrangian function. After 20 iterations, we found a solution of $12 081 574.76 which satisfies the stopping criterion (18). By applying the

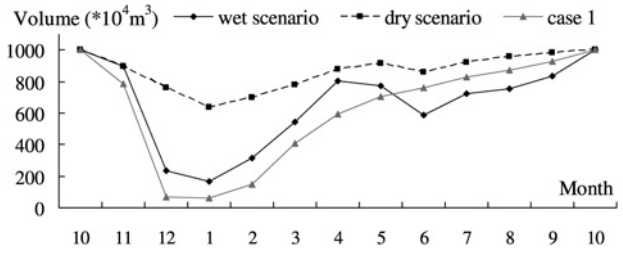

Fig. 6 *Terminal volumes at the end of each month*

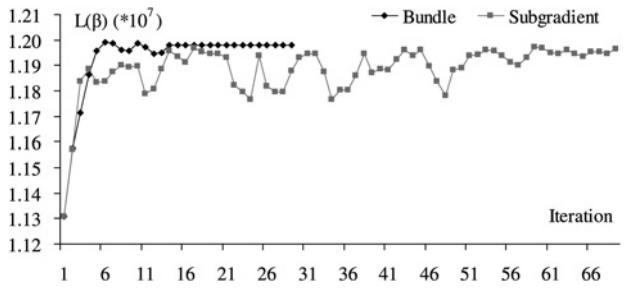

Fig. 7 *Iterative values of L(β) in Case 1*

heuristic adjustments (20)–(22), the final social cost is $12 141 356.75. Fig. 7 shows the better performance of bundle method in comparison with that of the subgradient method. Fig. 8 shows the degree of constraints violation as calculated in (19). The violation in bundle method is reduced much faster than that in the subgradient method, implying that the feasibility is further improved. A better schedule is obtained, which needs less modification in the heuristics process for deriving a final feasible solution.

3.2 IEEE 118-bus system

A modified IEEE 118-bus system is studied with 54 fossil units, 12 gas-fired units, 7 hydro units, 186 branches and 91 demand sides. The peak load is 8600 MW. Hydro units

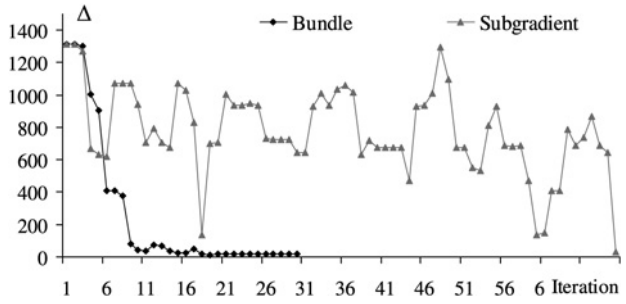

Fig. 8 *Iterative values of reservoir coupling violation in Case 1*

Table 8 Weight of each scenario after scenario reduction

Scenario	1	2	3	4	5	6
weight	0.05	0.075	0.125	0.07	0.09	0.185
Scenario	7	8	9	10	11	12
weight	0.065	0.07	0.06	0.05	0.05	0.11

Table 9 Results for the first 3 months of Case 1

Social cost, $			167 505 857.79
load shedding, MWh			5815.99
volume at the end of each month, $\times 10^4$ m^3	hydro unit 1	11	789.521400
		12	100.576885
		1	70
	hydro unit 5	11	814.661521
		12	110.595936
		1	60

Table 10 Results in the following seasons based on results of Case 1

Scenario	Social cost, $	LS, MWh	Scenario	Social cost, $	LS, MWh
1	469 781 501.38	9623.66	7	551 316 220.46	8995.90
2	546 776 969.21	12 474.30	8	444 484 699.84	9254.63
3	475 292 113.82	9213.25	9	449 050 768.81	10 892.67
4	482 963 151.36	10 474.21	10	472 859 825.43	10 474.37
5	480 598 672.06	9264.79	11	579 381 075.70	8973.25
6	555 092 475.68	11 376.21	12	438 829 845.99	10 203.03
expected cost		498 438 128.63		expected LS	10 220.87

Table 11 Results of Case 2

First-stage solution (November)					
Social cost				$54 915 796.54	
LS, MWh				1641.65	
Terminal volume ($\times 10^4 m^3$)			Hydro unit 1		Hydro unit 5
			443.985		524.97
Second-stage solution (December–October)					
Scen	Social cost, $	LS, MWh	Scen	Social cost, $	LS, MWh
1	569 348 058.64	12 709.49	7	638 250 719.88	12 140.42
2	631 623 855.91	15 675.10	8	553 314 423.24	12 541.41
3	575 609 207.51	12 374.16	9	548 171 522.09	14 049.00
4	573 665 664.86	13 381.57	10	579 617 496.76	13 207.50
5	571 984 423.07	12 647.78	11	659 318 818.53	12 121.87
6	639 399 045.85	14 535.15	12	539 828 573.25	13 165.35
expected cost		592 150 917.73	expected LS		13 346.51

1–4 belong to one catchment and units 5–7 belong to the second catchment. Detailed generator, transmission line and gas network data are found in [12, 16]. For the 118-bus system, since it is impossible to run a monthly SCUC at one shot, each period refers to a time span of one week. Thus, the first stage contains four periods and the second stage contains remaining 48 periods in each scenario. The probability of each scenario is shown in Table 8. The same two cases in the 6-bus system are considered again. Tables 9 and 10 present the solution of Case 1 with a social cost of $167 505 857.79 for the winter season. Without considering the water inflow uncertainty, terminal reservoir volumes are limited to their corresponding minimum values. Adopting these terminal volumes as initial conditions for the following seasons, the future social cost is $498 438 128.63 with the load shedding of 10 220.87 MWh. Table 11 shows the optimal two-stage stochastic solution with uncertainties. The load shedding is reduced from 16 036.86 to 14 988.16 (i.e. 1641.65 + 13 346.51) MWh. The optimal allocation of water reservoirs for the midterm horizon reduces the social cost by 2.83% [i.e. ((498 438 128.63 + 167 505 857.79) − (54 915 796.54 + 592 150 917.73)) / (498 438 128.63 + 167 505 857.79)] which shows that by considering uncertainties in the optimisation of water and gas usages in a midterm horizon, one can optimally allocate water resource to enhance the system reliability.

4 Conclusions

This paper proposed a two-stage stochastic programming model for the optimisation of midterm water and gas usage with uncertainties. The probabilistic reliability criteria, which are measured by the expected load shedding quantity and number of hours that load shedding happens, are incorporated into the midterm stochastic UC problem, in which both the power and the gas network security constraints are checked. The optimal midterm water usage allocation is achieved by introducing reservoir operation rules with a global operation parameter for the whole catchment. The optimal operating point is based on the minimum social cost which includes operating and load shedding costs. The contributions of this work resides in the formulation of midterm hydro reservoir operation, the optimisation and coordination for the midterm water and natural gas usages, and the proposed solution methodology for the complex midterm scheduling problem by fully utilising the capabilities of state-of-the-art mixed-integer programming, Lagrangian relaxation, and BD techniques. The optimal point is influenced by the unavailability of power system components, power and gas load levels, and water inflows, which are accurately simulated via multiple scenarios by the MC method. The results reveal that water management policies have a major impact on the system reliability. The system reliability is significantly improved by efficiently adjusting the water usage in a midterm horizon. In this regard, the water usage is optimally distributed throughout the midterm horizon. The study shows that the proposed two-stage stochastic optimisation model can improve the power system reliability and decrease the social cost by optimally allocating water and gas usages in a midterm horizon.

5 Acknowledgment

This work was suppoted in part by the NSF grant ECCS-0801853.

doi: 10.1049/iet-gtd.2010.0215

6 References

1 Shahidehpour, M., Yamin, H., Li, Z.Y.: 'Market operations in electric power systems' (John Wiley & Sons, Inc., New York, 2002)
2 Arvanitidis, N.V., Rosing, J.: 'Composite representation of a multireservoir hydroelectric power system', *IEEE Trans. Power Appar. Syst.*, 1970, **89**, (2), pp. 319–326
3 Arvanitidis, N.V., Rosing, J.: 'Optimal operation of multireservoir systems using a composite representation', *IEEE Trans. Power Appar. Syst.*, 1970, **89**, (2), pp. 327–335
4 Yu, Z., Sparrow, F.T., Bowen, B.H.: 'A new long-term hydro production scheduling method for maximizing the profit of hydroelectric systems', *IEEE Trans. Power Syst.*, 1998, **13**, (1), pp. 66–71
5 Labadie, J.W.: 'Optimal operation of multireservoir systems: state-of-the-art review', *J. Water Resour. Plan. Manage.*, 2004, **130**, (2), pp. 93–111
6 Shahidehpour, M., Fu, Y., Wiedman, T.: 'Impact of natural gas infrastructure on electric power systems', *IEEE Proc.*, 2005, **93**, (5), pp. 1042–1056
7 Lu, B., Shahidehpour, M.: 'Short-term scheduling of combined cycle units', *IEEE Trans. Power Syst.*, 2004, **19**, (3), pp. 1616–1625
8 Munoz, J., Jimenez-Redondo, N., Perez-Ruiz, J., Barquin, J.: 'Natural gas network modeling for power systems reliability studies'. Proc. IEEE/PES General Meeting, 2003, vol. 4, pp. 23–26
9 An, S., Li, Q., Gedra, T.W.: 'Natural gas and electricity optimal power flow'. Proc. IEEE/PES Transmission and Distribution Conf. Exposition, 2003, vol. 1, pp. 7–12
10 Morais, M.S., Marangon Lima, J.W.: 'Natural gas network pricing and its influence on electricity and gas markets'. 2003 IEEE Bologna PowerTech Conf., Bologna, Italy, 23–26 June
11 Li, T., Shahidehpour, M.: 'Interdependency of natural gas network and power system security', *IEEE Trans. Power Syst.*, 2008, **23**, (4), pp. 1817–1824
12 Liu, C., Shahidehpour, M., Li, Z., Fotuhi-Firuzabad, M.: 'Security-constrained unit commitment with natural gas transmission constraints', *IEEE Trans. Power Syst.*, 2009, **24**, (3), pp. 1523–1536
13 Staschus, K., Bell, A., Cashman, E.: 'Usable hydro capacity and electric utility production simulation and reliability calculations', *IEEE Trans. Power Syst.*, 1990, **5**, (2), pp. 531–538
14 Wu, L., Shahidehpour, M., Li, T.: 'Cost of reliability analysis based on stochastic unit commitment', *IEEE Trans. Power Syst.*, 2008, **23**, (3), pp. 1364–1374
15 Billinton, R., Allan, R.: 'Reliability evaluation of power systems' (Plenum Publishing Corporation, New York, London, 1996, 2nd edn.)
16 Wu, L., Shahidehpour, M., Li, T.: 'Stochastic security-constrained unit commitment', *IEEE Trans. Power Syst.*, 2007, **22**, (2), pp. 800–811
17 Wu, L., Shahidehpour, M., Li, Z.: 'GENCO's risk-constrained hydrothermal scheduling', *IEEE Trans. Power Syst.*, 2008, **23**, (4), pp. 1847–1858
18 Paul, G.: 'Monte carlo method in financial engineering' (Springer, New York, 2003)
19 Terry, L.A., Pereira, M.V.F., Neto, T.A.A., Silva, L.F.C.A., Sales, P.R.H.: 'Coordinating the energy generation of the Brazilian national hydrothermal electrical generating system', *Interfaces*, 1986, **16**, (1), pp. 16–38
20 Soares, S., Carneiro, A.A.F.M.: 'Reservoir operation rules for hydroelectric power system optimization'. 93 Proc. Joint Int. Power Conf. Athens Power Tech. , 1993, vol. 2, pp. 965–969
21 Williams, H.P.: 'Model building in mathematical programming' (John Wiley & Sons, 1999, 4th edn.)
22 Beale, E.M.L., Tomlin, J.A.: 'Special facilities in a general mathematical programming system for non-convex problems using ordered sets of variables'. Proc. Fifth Int. Conf. on Operations Research, Tavistock, London, 1969
23 Hiriart-Urruty, J.-B., Lemaréchal, C.: 'Convex analysis and minimization algorithm' (Springer-Verlag, 1993), vol. 2
24 Schramm, H., Zowe, J.: 'A version of the bundle idea for minimizing a nonsmooth function: conceptual idea, convergence analysis, numerical results', *SIAM J. Optim.*, 1992, **2**, (1), pp. 121–152